

Instantons and distribution functions of quarks in the nucleon

A. E. Dorokhov and N. I. Kochelev

N. N. Bogolyubov Theoretical Physics Laboratory, Joint Institute for Nuclear Research, 141980 Dubna, Moscow Region, Russia

Fiz. Elem. Chastits At. Yadra **26**, 5–31 (January–February 1995)

Recent advances in theory and experiment in deep inelastic scattering of polarized particles are reviewed. It is argued that fundamental nonperturbative properties of the QCD vacuum will provide the solution to the “spin crisis.” © 1995 American Institute of Physics.

INTRODUCTION

For several years, the problem of nucleon spin has been one of the most delicate issues in the modern theory of the strong interactions—quantum chromodynamics (QCD) (see the reviews of Refs. 1–5). Although anomalous spin effects in strong interactions were discovered long ago,^{6–8} a real explosion of interest in spin effects in QCD occurred after the EMC measurement⁹ of the fraction of the proton helicity that is carried by quarks:

$$\Delta\Sigma = 0.120 \pm 0.094 \pm 0.138. \quad (1)$$

Analysis of the data led to the conclusion that the sum of the quark helicities within the proton has a value comparable with zero ($\Delta\Sigma \approx 0$). This result led to a crisis of the naive parton model of the nucleon, in which all the helicity of the proton is carried by valence quarks.

The present review is devoted to the current status of theory and experiment in high-energy spin physics. We believe that it is impossible at the present time to give a definitive review of this very rapidly developing field in strong interactions, and therefore we merely attempt to discuss just some of the experiments and theoretical approaches in this field that we think are the most important.

POLARIZED DEEP INELASTIC SCATTERING (PDIS)

Kinematics of PDIS

The PDIS cross section (Fig. 1) for scattering of a polarized lepton on a polarized proton can be written in the form

$$d\sigma = \frac{\alpha^2}{\pi q^4} L_{\mu\nu} W_{\mu\nu} \frac{d^3k'}{(pk)E'},$$

where E and E' are the energies of the initial and final leptons, respectively, $q^2 = -4EE' \sin^2(\theta/2)$,

$$L_{\mu\nu} = u_l(k) \gamma_\mu u_l(k') \bar{u}_l(k') \gamma_\nu u_l(k),$$

is the well-known lepton tensor, and

$$W_{\mu\nu} = \frac{1}{4} \sum_n \langle p, \xi | J_\mu^{el}(0) | n \rangle \langle n | J_\nu^{el}(0) | p, \xi \rangle (2\pi)^4 \delta^4 \times (p + q - p_n). \quad (2)$$

In (2), ξ is the proton polarization vector, the summation is over all possible intermediate hadronic states n , and $J_\mu^{el}(x)$ is the hadronic electromagnetic current. In the quark model,

$$J_\mu^{el}(x) = \sum_{i=u,d,s,\dots} e_i \bar{q}_i(x) \gamma_\mu q_i(x).$$

The most general form of $W_{\mu\nu}$ that is consistent with the requirements of gauge and also P and T invariance is

$$\begin{aligned} \frac{1}{\pi} W_{\mu\lambda}(q, p, s) = & \left(g_{\mu\lambda} + \frac{q_\mu q_\lambda}{q^2} \right) W_1(\nu, Q^2) + \frac{1}{M^2} \\ & \times \left(p_\mu - \frac{\nu q_\mu}{q^2} \right) \left(p_\lambda - \frac{\nu q_\lambda}{q^2} \right) W_2(\nu, Q^2) \\ & + \frac{i}{M} \varepsilon_{\mu\lambda\rho\sigma} q_\rho \left(s_\sigma G_1(\nu, Q^2) \right. \\ & \left. + \frac{\nu}{M^2} G_2(\nu, Q^2) \right) \\ & - \frac{(sq)p_\sigma}{M^2} G_2(\nu, Q^2), \end{aligned} \quad (3)$$

where M is the proton mass, s is its spin, $Q^2 = -q^2$, and $\nu = (pq)$. The structure functions W_1 and W_2 determine the cross section of deep inelastic scattering (DIS) of unpolarized particles, and the spin-dependent structure functions G_1 and G_2 give information about the distribution of the spin between the charged constituents of the proton. In the Bjorken limit ($\nu, Q^2 \rightarrow \infty, x = Q^2/2\nu \rightarrow \text{const}$) in QCD scaling must hold (apart from logarithmic corrections):

$$W_1(\nu, Q^2) \equiv F_1(x, Q^2) \xrightarrow{\nu, Q^2 \rightarrow \infty} F_1(x),$$

$$\frac{\nu}{M^2} W_2(\nu, Q^2) \equiv F_2(x, Q^2) \xrightarrow{\nu, Q^2 \rightarrow \infty} F_2(x),$$

$$\frac{\nu}{M^2} G_1(\nu, Q^2) \equiv g_1(x, Q^2) \xrightarrow{\nu, Q^2 \rightarrow \infty} g_1(x),$$

$$\frac{\nu^2}{M^4} G_2(\nu, Q^2) \equiv g_2(x, Q^2) \xrightarrow{\nu, Q^2 \rightarrow \infty} g_2(x).$$

Experiment

In PDIS experiments, the asymmetry of the scattering of polarized leptons by polarized hadronic targets is measured. Thus, in the EMC experiment⁹ scattering of longitudinally polarized μ mesons on longitudinally polarized protons was used to measure the asymmetry

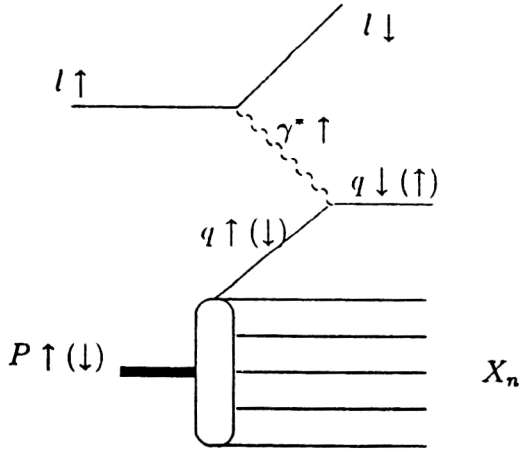


FIG. 1. Contribution to $g_1(x)$ in the framework of the quark-parton model of scattering of a longitudinally polarized lepton on a longitudinally polarized nucleon.

$$A_1(x, Q^2) = \frac{d\sigma^{\uparrow\downarrow} - d\sigma^{\uparrow\uparrow}}{d\sigma^{\uparrow\downarrow} + d\sigma^{\uparrow\uparrow}}, \quad (4)$$

where the arrows indicate the relative orientations of the proton and μ -meson spins.

By means of the expressions (2)–(4), this asymmetry can be readily related to the ratio of the spin-dependent proton structure functions to the spin-independent function (see, for example, Ref. 10):

$$A_1(x, Q^2) = 2x(1 + R(x, Q^2)) \frac{g_1(x, Q^2) - \gamma^2 g_2(x, Q^2)}{F_2(x, Q^2)}, \quad (5)$$

where $\gamma = Q^2/\nu^2$, and $R(x, Q^2)$ is the ratio of the cross sections for the absorption of longitudinal and transverse photons on the nucleon. At high energies, the contribution of

$g_2(x, Q^2)$ to (5) can be ignored, and the relation (5) makes it possible to determine the structure function $g_1^p(x)$.

In Fig. 2 we present data on $g_1^p(x, Q^2)$ obtained by the EMC, SMC, and E-143 collaborations.^{9,11,12} In the analysis of the experimental results, it is usual to discuss the value of the first moment of the structure function $g_1^p(x, Q^2)$:

$$\Gamma_1^p(Q^2) = \int_0^1 g_1^p(x, Q^2) dx, \quad (6)$$

which in the parton model (see below) can be related to the helicities of the quarks in the hadron. Here, two problems arise. The first is associated with the need to calculate $g_1^p(x, Q^2)$ at some fixed value of Q^2 from the available experimental data on $A_1(x, Q^2)$ in different Q^2 intervals. It is usual to make use of the assumption that $A_1(x, Q^2) \approx \text{const}(Q^2)$, which is confirmed by calculations in perturbative QCD.¹³ However, the experimental SMC data¹¹ on the asymmetries in the region of small x are not sufficient to permit a definite conclusion to be drawn concerning the validity of such an assumption.

The second problem is associated with the extrapolation to the experimentally inaccessible regions of x values: $x \rightarrow 0$ and $x \rightarrow 1$. The ambiguity in the extrapolation to the region $x \rightarrow 1$ usually does not give large errors in $\Gamma_1^p(Q^2)$, since, first, in this region the simple quark model of the nucleon with three valence quarks, in which $A_1(x, Q^2) \rightarrow 1$ as $x \rightarrow 1$ (Ref. 14), works well, and, second, the structure function $g_1^p(x, Q^2)$ itself must decrease rapidly, $\propto (1-x)^3$, as $x \rightarrow 1$.

The main problem is associated with the extrapolation to the region $x \rightarrow 0$. In this region, it is customary to use the Regge asymptotic form for $g_1^p(x, Q^2)$:

$$g_1^p(x) \rightarrow \frac{1}{x^{\alpha_{A_1}}}, \quad (7)$$

where $\alpha_{A_1} \approx 0$ is the intercept of the A_1 -meson trajectory. However, the recent SMC data at small values of x do not

Proton - World Data

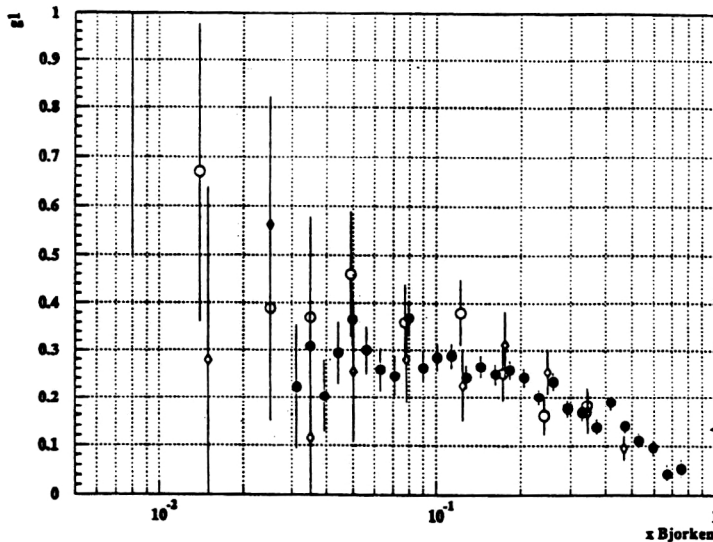


FIG. 2. Data on measurement of the structure function $g_1^p(x)$ obtained by the EMC, SMC, and E-143 collaborations.

indicate a transition to the asymptotic behavior as $g(x) \xrightarrow{p} \text{const}$ as $x \rightarrow 0$ (Fig. 1). There are also theoretical indications¹⁵ of possible deviations from (7) in the region of sufficiently small x .

With these assumptions, the latest experimental data for the first moments $g_1^p(x, Q^2)$ for the proton, neutron, and deuteron are

$$\begin{aligned} \text{EMC: } \Gamma_1^2(\langle Q^2 \rangle = 10.7 \text{ GeV}^2) &= 0.123 \pm 0.013 \pm 0.019, \\ \text{SMC: } \Gamma_1^p(\langle Q^2 \rangle = 10 \text{ GeV}^2) &= 0.136 \pm 0.011 \pm 0.011, \\ \Gamma_1^D(\langle Q^2 \rangle = 4.6 \text{ GeV}^2) &= 0.049 \pm 0.044 \pm 0.032, \\ \text{E-143: } \Gamma_1^p(\langle Q^2 \rangle = 3 \text{ GeV}^2) &= 0.129 \pm 0.004 \pm 0.010, \\ \Gamma_1^n(\langle Q^2 \rangle = 3 \text{ GeV}^2) &= -0.035 \pm 0.0096 \pm 0.011, \\ \Gamma_1^D(\langle Q^2 \rangle = 3 \text{ GeV}^2) &= 0.043 \pm 0.004 \pm 0.008, \end{aligned} \quad (8)$$

where we give the statistical and systematic errors. We mention here that the value for the integral for the neutron structure function was extracted from deuteron data. It was shown in Refs. 16 and 17 that in such an analysis accurate allowance must be made for nuclear effects.

PROTON SPIN IN PERTURBATIVE QCD

The idea behind the EMC, SMC, E-142, and E-143 experiments is simple. A muon of definite helicity emits a virtual γ^* photon, which also has definite helicity. A quark in the proton having spin projection $\pm 1/2$ onto the direction of motion of the muon can, depending on the sign of the projection, absorb a γ^* photon only of definite helicity. Therefore, in measuring the difference of the cross sections in (4), we do indeed measure the distribution of the charged protons with respect to the helicity within the proton. Consequently, in the quark-parton model the structure function $g_1^p(x)$ can be expressed in terms of the helicity distribution functions of the quarks within the proton. Using Fig. 1, it is easy to obtain the contribution of scattering of the virtual γ^* photon on a massless quark with helicity $(1/2)S_i$ to the antisymmetric part of the tensor (3):

$$\begin{aligned} W_{\mu\lambda}^{i,A} &= e_i^2 \delta((k+q)^2) \text{Tr}((1 - \gamma_5 S_i) \not{k} \gamma_\mu (\not{k} + \not{q}) \gamma_\lambda) \\ &= i e_i^2 2\nu \delta(x - Q^2/2\nu) S_i \varepsilon_{\mu\lambda\rho\sigma} q_\rho k_\sigma. \end{aligned}$$

Comparing this with (3), we obtain

$$g_q^p(x) = \frac{1}{2} \sum_i e_i^2 (q_+^i(x) - q_-^i(x)) = \frac{1}{2} \sum_i e_i^2 \Delta q_i(x), \quad (9)$$

where q_+^i and q_-^i are the probabilities of a quark of species i having helicity along the proton helicity and in the opposite direction.

Thus, in the quark-parton model the integral $\Gamma_1^p(Q^2)$ can be expressed in terms of the helicity carried by the quarks of the different species in the proton:

$$\begin{aligned} \Gamma_1^p(Q^2) &= \frac{1}{12} (\Delta u - \Delta d) + \frac{1}{36} (\Delta u + \Delta d - 2\Delta s) \\ &\quad + \frac{1}{9} (\Delta u + \Delta d + \Delta s), \end{aligned} \quad (10)$$

where

$$\Delta q_i = \int_0^1 \Delta q_i(x) dx. \quad (11)$$

For the integral of the neutron structure function $g_1^n(x, Q^2)$, we obtain an analogous expression, differing only in the sign of the first term in (10).

On the other hand, the quantities (11) can be expressed in terms of the matrix elements of the axial-vector current:

$$\begin{aligned} \Delta q_i S_\mu &= \frac{1}{2} (\langle p, S | \bar{q}_i (1 + \gamma_5) \gamma_\mu q_i | p, S \rangle - \langle p, S | \bar{q}_i \\ &\quad \times (1 - \gamma_5) \gamma_\mu q_i | p, S \rangle) \\ &= \langle p, S | \bar{q}_i \gamma_5 \gamma_\mu q_i | p, S \rangle. \end{aligned} \quad (12)$$

Under the assumption of the validity of $SU_f(3)$ asymmetry of the wave functions of the baryon octet, some combinations of the matrix elements (12) can be expressed in terms of the constants of hyperon weak decays:

$$\Delta u - \Delta d = g_A^3 = F + D, \quad \Delta u + \Delta d - 2\Delta s = g_A^8 = 3F - D. \quad (13)$$

The latest fit of these constants gives the values

$$F/D = 0.575 \pm 0.016, \quad F + D = 1.257 \pm 0.03. \quad (14)$$

In QCD, allowance for exchange of perturbative gluons between the quarks changes the coefficients in (10). Significant progress was recently achieved in the calculation of the α_s corrections to the coefficient functions of the first moments of $g_1^p(x, Q^2)$ (Ref. 18). The modified expression is

$$\begin{aligned} \int_0^1 g_1^{p,n}(x, Q^2) dx &= \pm \frac{C_1(Q^2)}{12} (\Delta u - \Delta d) \\ &\quad + \frac{C_1(Q^2)}{36} (\Delta u + \Delta d - 2\Delta s) \\ &\quad + \frac{C_0(Q^2)}{9} (\Delta u + \Delta d + \Delta s), \end{aligned} \quad (15)$$

where

$$\begin{aligned} C_1(Q^2) &= 1 - \frac{\alpha_s(Q^2)}{\pi} - 3.58 \left(\frac{\alpha_s(Q^2)}{\pi} \right)^2 \\ &\quad - 20.22 \left(\frac{\alpha_s(Q^2)}{\pi} \right)^3, \\ C_0(Q^2) &= 1 - \frac{\alpha_s(Q^2)}{3\pi} - 0.55 \left(\frac{\alpha_s(Q^2)}{\pi} \right)^3. \end{aligned} \quad (16)$$

These corrections are very appreciable at small Q^2 and make it possible to explain an appreciable fraction of the difference in the results for $\Gamma_1^p(Q^2)$ and $\Gamma_1^n(Q^2)$ obtained by the EMC, SMC, E-142, and E-143 collaborations.¹⁹

Knowledge of these corrections to the Bjorken sum rule²⁰

$$\int_0^1 dx [g_1^p(x, Q^2) - g_1^n(x, Q^2)] = \frac{C_1(Q^2)}{6} g_A^3 \quad (17)$$

also gives a method for finding the value of $\alpha_s(Q^2)$ from data on the polarized structure functions.²¹

From analysis of the experimental data (8) and the expressions (15) and (16), using the values (14) for the proton helicity carried by the quarks,

$$\Delta\Sigma = \Delta u + \Delta d + \Delta s, \quad (18)$$

we obtain the world average value²¹

$$\Delta\Sigma = 0.33 \pm 0.04, \quad (19)$$

which is much lower than the predictions of the naive non-relativistic quark model,

$$\Delta\Sigma = 1. \quad (20)$$

In the studies of Ref. 22, analysis of the Gerasimov–Drell–Hearn sum rules²³ led to the conclusion that there could be a large contribution of higher twists to $\Gamma_1^p(Q^2)$, which would make it possible to reduce appreciably the difference between (19) and (20). Unfortunately, the model used in Ref. 22 does not have a direct relation to QCD, and therefore this suggestion requires verification. On the other hand, a calculation of the higher twists in accordance with QCD sum rules²⁴ leads to a very small contribution of them to $\Gamma_1^p(Q^2)$.

However, a serious shortcoming of this calculation was that it made no allowance at all for the contribution of the axial anomaly in the Q^2 dependence of the structure functions. In our view, at the present time not only the magnitude but even the sign of the higher-twist contributions to $\Gamma_1^p(Q^2)$ is undetermined, and this question requires more detailed experimental and theoretical investigation.

Allowance for $SU(3)_f$ breaking in the wave functions of the baryon octet can also change the value of (19). A more recent careful consideration of this question²⁵ showed that allowance for this breaking leads to a decrease in the value of $\Delta\Sigma$.

PROTON SPIN IN NONPERTURBATIVE QCD

As we have already noted above, the result (19) does not agree with the expectations of the nonrelativistic quark model, in which the entire proton spin is carried by the three valence quarks. Allowance for relativistic effects somewhat changes the value of $\Delta\Sigma$. This is due to the admixture of the state with orbital angular momentum $l=1$ in the wave function of a relativistic quark. Thus, the wave function of a quark moving in a scalar spherically symmetric potential has the form

$$\Psi_m = \begin{pmatrix} f(r)U_m \\ ig(r)\hat{\sigma}\hat{r}U_m \end{pmatrix}, \quad (21)$$

where U_m is the two-component spinor corresponding to the angular-momentum projection m , and f and g are functions that depend on the specific form of the potential. The two upper components of the four-component spinor correspond to the value $l=0$, and the two lower ones to $l=1$. The mean value of the quark spin projection is

$$\Delta\Sigma_q = \left\langle q \left| \int d^3x \bar{\Psi} \gamma_3 \gamma_5 \Psi \right| q \right\rangle = \frac{\int \left(f^2 - \frac{1}{3} g^2 \right) r^2 dr}{\int (f^2 + g^2) r^2 dr}. \quad (22)$$

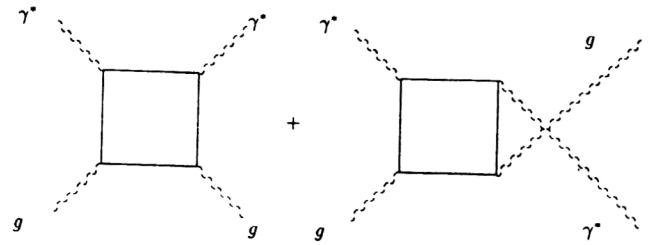


FIG. 3. Contribution of gluons to the structure function $g_1(x)$.

In the nonrelativistic limit $g=0$, and therefore $\Delta\Sigma=1$. In the relativistic case, we have $g \neq 0$, and the value of (22) is then determined by the form of the confinement potential. For example, the ultrarelativistic version of the popular bag model^{26,27} with massless quarks and with functions

$$f(r) = j_0(\chi r/R), \quad g(r) = j_1(\chi r/R), \quad \chi = 2.043,$$

gives

$$\Delta\Sigma^{\text{bag}} = 0.65, \quad (23)$$

and the inclusion of quark masses merely increases this value.

Thus, although allowance for relativistic effects does somewhat reduce the value of the helicity carried by the valence quarks of the proton, this reduction is not sufficiently great to explain the measured value (19). Therefore, the proton helicity is not determined by the spins of the valence quarks.

This conclusion casts doubt on many achievements of the constituent quark model (CQM) in the description of hadronic properties. The situation appeared so serious that it was called the “spin crisis.”²⁸ Several ways of solving the problem have been proposed.

One solution was found in Ref. 29, where it was shown that a small value of the matrix element of the isosinglet axial-vector current can be associated with the Adler–Bell–Jackiw axial anomaly,³⁰ which breaks its conservation:

$$\partial_\mu j_{\mu 5}^0 = 2 \sum_{i=1}^{N_f} m_i \bar{q}_i \gamma_5 q_i + \frac{N_f \alpha_s}{4\pi} G_{\mu\nu}^a \tilde{G}_{\mu\nu}^a. \quad (24)$$

The magnitude of the nonconservation is determined by the matrix element

$$M = \left\langle p, s \left| \frac{\alpha_s}{8\pi} G_{\mu\nu}^a \tilde{G}_{\mu\nu}^a \right| p, s \right\rangle, \quad (25)$$

which is the main object of study of many approaches based on QCD.

There are two approaches to the problem of taking into account the contributions of the gluon anomaly to the spin-dependent structure functions. One of them, which we shall nominally call the perturbative approach, relates the contribution of the axial anomaly to the polarization of the gluons in the hadron wave function. In this approach, the contribution of the axial anomaly to the structure function $g_1^p(x)$ is determined by the diagrams shown in Fig. 3.

By means of the theorem on the factorization of large and small distances,³¹ this contribution can be represented in the form

$$\Delta g_1^p(x, Q^2) = \left\langle \frac{e^2}{2} \right\rangle A^{\text{hard}}(x, Q^2/\mu^2) \otimes \Delta g(x, \mu^2), \quad (26)$$

where $A^{\text{hard}}(x, Q^2/\mu^2)$ is the cross section of the perturbative subprocess calculated using the diagrams of Fig. 3, $\Delta g(x, \mu^2)$ is the distribution function of the gluons with respect to the helicity in the nucleon, and μ^2 is the scale at which the factorization of the large and small distances is made. In (26), the symbol \otimes denotes a convolution:

$$A(x) \otimes \Delta g(x) \equiv \int_x^1 \frac{dy}{y} A\left(\frac{x}{y}\right) \Delta g(y).$$

As a result, the effect of the anomaly reduces to replacement of the quark distributions by the combination

$$\Delta \tilde{q} = \Delta q - \frac{\alpha_s}{2\pi} \Delta G. \quad (27)$$

Unfortunately, a more careful study³² showed that the decomposition (26) depends on the infrared-cutoff parameter in the integral (26), and this makes the physical interpretation of the expression (27) difficult.

A different approach to allowance for the contributions of the axial anomaly in processes of interaction of polarized particles is being actively developed by the authors of this review and involves allowance for the contributions of strong fluctuations of the gluon fields—instantons³³—to the quark distribution functions. The instanton mechanism for solution of the “spin crisis” was proposed almost simultaneously in Refs. 34 and 35. The idea was that the gluon operator in the matrix element (25), which determines the degree of nonconservation of the isosinglet axial-vector current,

$$Q(x) = \frac{\alpha_s}{8\pi} G_{\mu\nu}^a(x) \tilde{G}_{\mu\nu}^a(x), \quad (28)$$

is the density operator of a topological charge, and therefore only topologically nontrivial fluctuations of the gluon fields can make a nonvanishing contribution to (25). In QCD, instantons are a well-known example of such fluctuations. This solution describes tunneling transitions between nontrivial degenerate vacuum states that have different values of the topological charge. From (24) it is readily found that the change of the axial charge is related to a change of the topological charge by the amount

$$\Delta Q_5 = 2N_f \Delta Q. \quad (29)$$

Therefore, when quarks are scattered on an instanton (anti-instanton) with $\Delta Q = \mp 1$, there is a change of their helicity by the amount

$$\Delta \Sigma_q = \Delta Q_5 = \mp 2N_f. \quad (30)$$

To find the matrix element (25) between the nucleon states, it is necessary to know the dynamics of the change of

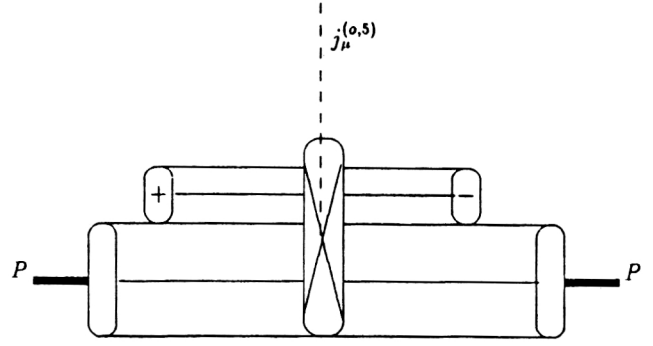


FIG. 4. Contribution of instantons to the matrix element of the singlet axial-vector current $j_\mu^{(0,5)}$.

the quark helicity in the instanton field. It is determined by the effective 't Hooft interaction,³⁶ which for small instantons ($\rho \rightarrow 0$) and $N_f = 2$ has the form

$$\begin{aligned} \mathcal{L}_{\text{eff}}(x) = & \int d\rho n(\rho) \left(\frac{4}{3} \pi^2 \rho^3 \right)^2 \bar{u}_R u_L \bar{d}_R d_L \left[1 + \frac{3}{32} \right. \\ & \times \left(1 - \frac{3}{4} \sigma_{\mu\nu}^u \sigma_{\mu\nu}^d \right) \lambda_u^a \lambda_d^a \left. \right] + (R \leftrightarrow L) \\ & + (d \rightarrow s) + (u \rightarrow s). \end{aligned} \quad (31)$$

The contribution of the instantons to the matrix element of the axial current is determined by the diagrams shown in Fig. 4. This contribution was first estimated with the wave functions of the bag model in Ref. 5. With allowance for only the five-quark component in the hadron wave function induced by instantons, it was found to be

$$\Delta \Sigma_I^s = -4N_f \left(\frac{\rho_c}{R} \right)^4 I, \quad (32)$$

where $\rho_c \approx 2 \text{ GeV}^{-1}$ is the mean scale of the instantons of the QCD vacuum (Ref. 37), $R \approx 5 \text{ GeV}^{-1}$, and I is the overlap integral of the wave functions of the initial three-quark and intermediate five-quark states.

Numerically, the result of the reduction of the quark helicity induced by the instantons is $\Delta \Sigma_{\text{bag}}^I = -0.04$. Although this quantity is small in absolute magnitude, it agrees in sign with the experimentally observed negative polarization of the sea quarks. However, the result is extremely sensitive to the form of the wave functions, and the use of the wave functions of the bag model with explicit nonconservation of quark helicity at the bag boundary is evidently a bad approximation.

In this connection, we mention the result of Ref. 38, in which a calculation was made of the reduction of the helicity of a free quark in the instanton vacuum for $N_f = 1$: $\Delta \Sigma_{N_f=1}^I = -1$. A calculation of the quark helicity induced by instantons with a realistic proton wave function obtained in the instanton vacuum model³⁷ is currently being made.³⁹

A small value of the matrix element of the singlet axial-vector current was also obtained in various versions of the Skyrme model.⁴⁰ It was also associated with nontrivial topological properties of the theory.

Recently, considerable progress has been made in the calculation of quark helicity in the framework of QCD sum rules.⁴¹ The authors of that work calculated the decay constant of the singlet η'_0 meson, $F_{\eta'_0}$, in the analog of the Goldberger–Treiman relation for the singlet channel:⁴²

$$G_A^{(0)}(0, Q^2) = \frac{F_{\eta'_0} g_{\eta'_0 NN}}{2M}, \quad (33)$$

where $g_{\eta'_0 NN} \approx \sqrt{2} g_{\eta'_0 NN}$ is the coupling constant of the η'_0 meson with the nucleon. This resulted in a large reduction of the quark helicity,

$$G_A^{(0)}(10 \text{ GeV}^2) = \Delta\Sigma = 0.353 \pm 0.052, \quad (34)$$

this being due to the decrease in $F_{\eta'_0}$ arising from the axial anomaly with respect to its OZI value $F_{\eta'_0 \text{OZI}} = f_\pi / \sqrt{6}$:

$$F_{\eta'_0} / F_{\eta'_0 \text{OZI}} \approx 0.6. \quad (35)$$

We note that a connection between the decrease in the value of $F_{\eta'_0}$ and the “spin crisis” was pointed out by us earlier in Ref. 43, in which we showed that

$$F_{\eta'_0} / F_{\eta'_0 \text{OZI}} \approx \frac{R_\pi}{R_{\eta'_0}} \approx 0.5. \quad (36)$$

In (36), R_π and $R_{\eta'_0}$ are the quark confinement radii in the π and η'_0 mesons. The difference between the meson radii arises because the instantons lead to a strong attraction of the quarks in the π meson and, in contrast, to a strong repulsion between the quarks in the η'_0 meson.⁴⁴

QUARK DISTRIBUTION FUNCTIONS IN THE INSTANTON VACUUM

One of the achievements of the instanton approach is the possibility of calculating not only the first moment of $g_i^q(x, Q^2)$ but also, more importantly, the x dependence of the distribution functions of the quarks with respect to the helicity and flavor. This opens up a unique possibility for simultaneous analysis of the spin-dependent and spin-independent structure functions in the framework of a single approach, since they are related by

$$\begin{aligned} \Delta q_i &= q_+(x) - q_-(x), \\ q_i &= q_+(x) + q_-(x). \end{aligned} \quad (37)$$

In perturbative QCD, a first attempt was also recently made at a simultaneous analysis of the spin-dependent and spin-independent structure functions.⁴⁵ However, the parametrization of the quark distribution functions in Ref. 45 contains very many free parameters, and this reduces the reliability of the predictions of this model. The same can also be said of the approach of Ref. 46, in which, however, in contrast to Ref. 45, the importance of taking into account the Pauli principle for the sea quarks in the parametrization of the structure functions was emphasized.

Unique properties of the interaction induced by instantons (Ref. 36, Fig. 5),

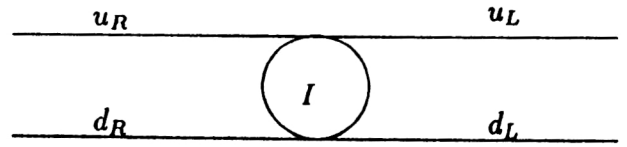


FIG. 5. Instanton-induced vertex in QCD.

$$\begin{aligned} \mathcal{L}_{\text{eff}}^{(N_f=2)}(x) &= f(|k_1|)f(|k_2|)f(|k_3|)f(|k_4|)\bar{u}_R u_L \bar{d}_R d_L \\ &\times \left[1 + \frac{3}{32} \left(1 - \frac{3}{4} \sigma_{\mu\nu}^a \sigma_{\mu\nu}^d \right) \lambda_u^a \lambda_d^a \right] \\ &+ (R \leftrightarrow L) + (d \rightarrow s) + (u \rightarrow s), \end{aligned} \quad (38)$$

are the following. First, this vertex leads to a very strong change of the quark helicities, $\Delta\Sigma = \pm 2N_f$; this gives us a fundamental mechanism for violating the Ellis–Jaffe sum rule⁴⁷ and resolving the “spin crisis.” Second, it is possible only between quarks of different flavors. We shall see below that this property leads to a strong flavor asymmetry of the quark sea and gives us a fundamental mechanism for the violation of the Gottfried sum rule⁴⁸ that was recently discovered⁴⁹ by the NMC collaboration. A third very important property of the vertex (38) is that it is pointlike for quarks on the mass shell. This leads to an anomalous growth of the quark–quark cross sections induced by instantons at high energies⁵⁰ and, accordingly, to an anomalous behavior of the quark distribution functions induced by instantons at low values of the Bjorken variable x (Ref. 51).

The instanton contribution to the distribution functions of the quarks in the proton is given by the diagrams shown in Fig. 6. Using an $SU(6)$ -symmetric wave function for the valence quarks in the proton,

$$p \uparrow = \frac{2}{3} u \uparrow + \frac{1}{3} u \downarrow + \frac{1}{3} d \uparrow + \frac{2}{3} d \downarrow \quad (39)$$

and the properties of the instanton vertex (38), we can obtain the instanton contributions to the spin-dependent distribution functions of the sea quarks,⁵²

$$2\Delta\bar{u}_I = f(x), \quad 2\Delta\bar{d}_I = -4f(x), \quad 2\Delta\bar{s}_I = -3\lambda_s f(x) \quad (40)$$

and the valence quarks,

$$\Delta u_I^v = -4f(x), \quad 2\Delta d_I^v = f(x), \quad (41)$$

where $\lambda_s \approx (m_u^*/m_s^*)^2 \approx 0.32$ is the suppression factor of the interaction induced by the instantons for the strange quarks in the model of an instanton liquid,³⁷ and $f(x)$ is a function determined by the dynamical properties of the interaction through the instantons. We can also find the flavor-dependent distributions of the sea quarks:

$$2\bar{u}_I = f(x), \quad 2\bar{d}_I = 2f(x), \quad 2\bar{s}_I = 3\lambda_s f(x). \quad (42)$$

From these relations, we obtain

$$\frac{\bar{d}_I}{\bar{u}_I} = 2, \quad \frac{2\bar{s}_I}{\bar{u}_I + \bar{d}_I} \approx 1, \quad (43)$$

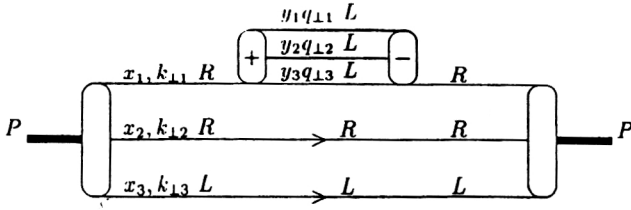


FIG. 6. Diagram representing the contribution of the five-quark configuration from the instanton-induced interaction to the proton wave function.

and therefore the instantons lead to a strong breaking of the $SU(2)_f$ symmetry of the quark sea in the proton and to an enhancement of its strangeness.

At the present time, there is much discussion of the reason for the large violation of the Gottfried sum rule,⁴⁸

$$\begin{aligned} & \int_0^1 (F_2^p(x) - F_2^n(x)) dx \\ &= \frac{1}{3} \int_0^1 (u_v(x) - d_v(x)) dx - \frac{2}{3} \int_0^1 (\bar{d}(x) - \bar{u}(x)) dx, \end{aligned} \quad (44)$$

found by the NMC collaboration:⁴⁹

$$\int_0^1 (\bar{d}(x) - \bar{u}(x)) dx = 0.11 \pm 0.02. \quad (45)$$

A similar violation of the relation $\bar{d} = 2\bar{u}$ for $\langle x \rangle \approx 0.18$ was also found by the NA51 collaboration from an analysis of data on the production of Drell–Yan pairs in pp and pD interactions.⁵³

The instanton model for the structure functions makes it possible to explain these results. Thus, it follows from the relations (40) and (42) that the polarization of the quark sea and the degree of its flavor asymmetry are related. This is in fact a manifestation of the Pauli principle for quarks in zero modes in the instanton field, from which the Lagrangian (38) is constructed. These relations were used in Ref. 51 to obtain a new parton sum rule that relates the violations of the Ellis–Jaffe and Gottfried sum rules:

$$\int_0^1 g_1^p(x) dx - \frac{5g_A^8 + 3g_A^3}{36} = \int_0^1 \frac{dx}{x} (F_2^p(x) - F_2^n(x)). \quad (46)$$

As was noted above, the most interesting thing would be to calculate the dependence of the anomaly contributions on the Bjorken variable x . In the instanton approach, the dependence is determined by the shape of the function $f(x)$. In the region $x \rightarrow 1$, the dominant contribution is made by the five-quark Fock component of the nucleon wave function⁵² (Fig. 6). In the infinite-momentum frame, the quark distribution functions are related to the proton wave function in the infinite-momentum frame by⁵⁴

$$\begin{aligned} q_{f/p}(x, k_\perp, Q^2) &= \int [dk_{\perp i}] [dx_i] \delta(x - x_q) \\ &\times |\Psi_{(5)}(k_{\perp i}, x_i)|^2 \Theta(k_{\perp i}^2 \leq Q^2). \end{aligned} \quad (47)$$

In the model of the QCD vacuum as an instanton liquid³⁷ there are two fundamental scales. One of them is the mean instanton size in the vacuum, $\rho_c \approx 2 \text{ GeV}^{-1}$, and the other is the separation between them: $R \approx 3\rho_c$. The first is related to the radius of a constituent quark, and the second to the confinement radius.

In Ref. 52, it was found that the existence of these two very different scales in QCD leads to a large asymmetry with respect to x_i and $k_{\perp i}$ for the quark configurations in the hadron wave function induced by the instantons. This can be shown as follows. The contribution of the diagrams of Fig. 6 in the framework of perturbation theory in the infinite-momentum frame is given by⁵²:

$$\begin{aligned} & |\Psi_5(k_{\perp i}, x_i; q_{\perp j}, y_j)|^2 \\ & \sim \frac{\Gamma_p(k_{\perp i}, x_i) \Gamma_I(q_{\perp j}, y_j) (\sum_j q_j^2)^{2l}}{\left(M_p^2 - \sum_{i=1}^3 \frac{k_{\perp i}^2 + m_i^2}{x_i} \right)^2 \left(\frac{k_{\perp 1}^2 + m_1^2}{x_1} - \sum_{j=1}^3 \frac{q_{\perp j}^2 + m_j^2}{y_j} \right)^2}, \end{aligned} \quad (48)$$

where Γ_p and Γ_I are the proton and instanton form factors, respectively, which can be approximated by the relations:

$$\begin{aligned} \Gamma_p(k_{\perp i}, x_i) &= \exp \left\{ -\frac{R^2}{6} \sum_{i=1}^3 \frac{k_{\perp i}^2 + m_i^2}{x_i} \right\} \quad R \approx 5 \text{ GeV}^{-1}, \\ \Gamma_I(q_{\perp j}, y_j) &= \exp \left\{ -\frac{\rho_c^2}{6} \sum_{j=1}^3 \frac{q_{\perp j}^2 + m_j^2}{y_j} \right\} \quad \rho_c \approx 2 \text{ GeV}^{-1}. \end{aligned} \quad (49)$$

Substituting (48) in (47), we can find the distribution functions of the quarks with respect to x_i and with respect to $k_{\perp i}$ in the nucleon.

It follows directly from the relation $\langle q_{\perp}^2 \rangle^{\text{inst}} / \langle k_{\perp}^2 \rangle^{\text{conf}} \approx R^2 / \rho_c^2 \approx 10$ that the mean transverse momentum of the quarks produced by an instanton fluctuation, $\langle k_{\perp}^2 \rangle^{\text{inst}} \sim 1 \text{ GeV}^2$, is much greater than the mean transverse quark momentum in the confinement potential, $\langle k_{\perp}^2 \rangle^{\text{conf}} \sim 0.1 \text{ GeV}^2$.

The asymmetry in the distribution with respect to the transverse momenta leads, in its turn, to a strong asymmetry in the distribution with respect to the longitudinal momenta. This is due to the fact that the main contribution to the integral (47) is made by the region

$$\frac{q_{\perp j}^{\text{inst}}}{y_j} \approx \frac{k_{\perp i}^{\text{conf}}}{x_i} \approx \text{const}, \quad (50)$$

which corresponds to the condition of equality of the quark rapidities in the multi-quark configuration in the nucleon wave function. In other words, the condition (50) corresponds to a coherent motion of the quarks in the nucleon for which the nucleon does not disintegrate. From the relation (50) it follows that $\langle y_j^{\text{inst}} \rangle \approx 3 \langle x_i \rangle^{\text{conf}}$ and that the quark sea

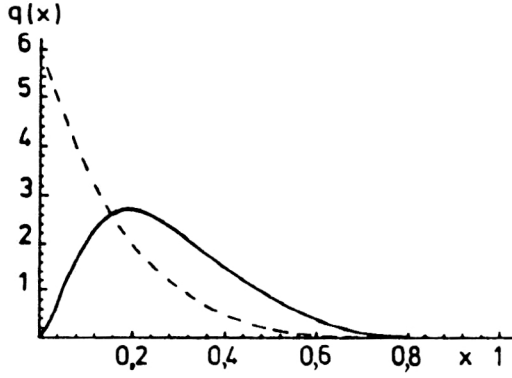


FIG. 7. Longitudinal-momentum distribution of “fast” (solid curve) and “slow” (dashed curve) quarks in the asymmetric configuration of the proton wave function induced by instantons.

induced by the instantons is hard.⁵² The actual form of the quark distribution functions in this asymmetric configuration for the instanton-produced quarks is

$$q^{\text{hard}}(x) = N \{ (1-x)^2 x^2 / 2 + 6(1-x)x^3 - 8 \times (1-x)^{1/2} x^3 (1+5x) \operatorname{arctanh}[(1-x)^{1/2} / (1+3x)^{1/2}] / (1+3x)^{1/2} + 24x^4 (\operatorname{arctanh} [(1-x)^{1/2} / (1+3x)^{1/2}])^2 \}, \quad (51)$$

and for quarks that have not passed through an instanton it is

$$q^{\text{soft}}(x) = N[(1-x)^5 (159 - 32 \log 4)] / 4860. \quad (52)$$

The two distributions are compared in Fig. 7.

Thus, the instantons lead to hard sea quark distribution functions, which must make large contributions to the inclusive production of particles for $x_F \rightarrow 1$ and $p_\perp \geq 1$ GeV, where the contributions of the perturbative sea die out. In particular, the instanton-induced charmed sea can provide a model of internal charm in the nucleon, the need for the introduction of which is currently being actively discussed.⁵⁸

The diffraction component in the instanton-induced hadron wave function must also lead to an anomalous nuclear dependence of the hadronic inclusive cross sections for $x_F \rightarrow 1$ and $p_\perp \geq 1$ GeV and to a violation of color transparency.⁵⁵ Since this component also has a spin dependence, it was shown in Ref. 55 that the same-spin asymmetries in the processes $p \uparrow A \rightarrow \pi X$ must also have an anomalous A dependence.

A calculation of the structure functions requires a knowledge of the quark distribution functions in the complete interval of x . However, in the region $x \rightarrow 0$ the situation is much more complicated than in the region $x \rightarrow 1$, since here it is necessary to take into account the contributions of multi-gluon and multi-quark configurations of the Fock column in the nucleon wave function.

In this region, the behavior of the distribution functions can be related to the behavior of the quark-quark cross sections at high energies⁵¹ (see Fig. 8):

$$q(x) = C \frac{x}{1-x} \int ds dk_\perp^2 \operatorname{Im} T_R^N(s, \mu^2), \quad (53)$$

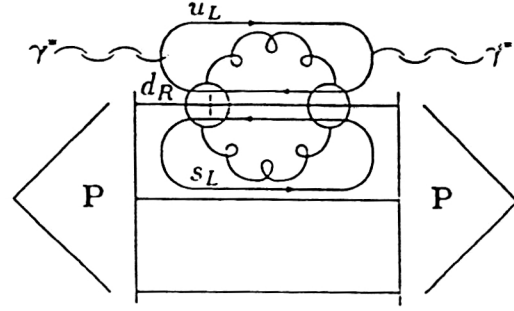


FIG. 8. Contribution to the nucleon structure function as $x \rightarrow 0$ resulting from the instanton mechanism of generation of the quark sea (the + and - signs represent an instanton and an anti-instanton).

where $T_R^N(s, \mu^2)$ is the quark-nucleon scattering amplitude, and

$$\mu^2 = -x \frac{(s + k_\perp^2)}{1-x} + xM^2 - k_\perp^2. \quad (54)$$

Thus, it follows from this relation that if the amplitude factorizes in the form

$$\operatorname{Im} T_R^N(s, \mu^2) \sim \sigma_{q\bar{q}}(s) f(\mu^2), \quad (55)$$

where $\sigma_{q\bar{q}} \sim s^{\alpha-1}$, then the distribution functions in the region of small x are

$$q(x \rightarrow 0) \sim \frac{1}{x^\alpha}. \quad (56)$$

Thus, the anomalous behavior of the quark-quark cross sections at high energies leads to an anomalous behavior of the structure functions at small x .

At the present time, there is much discussion of electroweak instantons in processes of baryon-number nonconservation in electroweak theories.⁵⁰ For example, it was shown that multiple production of gauge bosons from an instanton vertex can lead to an anomalous growth of the cross sections with nonconservation of the baryon number. Obviously, this is due to the pointlike nature of the instanton interaction noted above.

A similar mechanism also leads to an anomalous growth of the instanton-induced cross sections in QCD.⁵⁶ In the studies of Ref. 57, the contribution of small instantons to the coefficient function of the structure function F_2 was calculated. It is determined by the action $S(x)$ on the instanton-anti-instanton configuration,

$$\delta F_2^I(x, Q^2) \sim \exp[-4\pi S(x)/\alpha_s(Q^2)], \quad (57)$$

where

$$S(x) \approx 1 - 3(1-x)^2 / 2(1+x)^2.$$

Although the instanton contribution increases exponentially with decreasing x , at $Q_0 > 50$ GeV, where the calculations in the approximation of a rarefied instanton gas are valid, this contribution is the contribution of a very high fractional twist $\sim (\Lambda_{\text{QCD}}^2 / Q^2)^{9S(x)}$ to the structure function, and therefore these results are evidently only of academic interest.

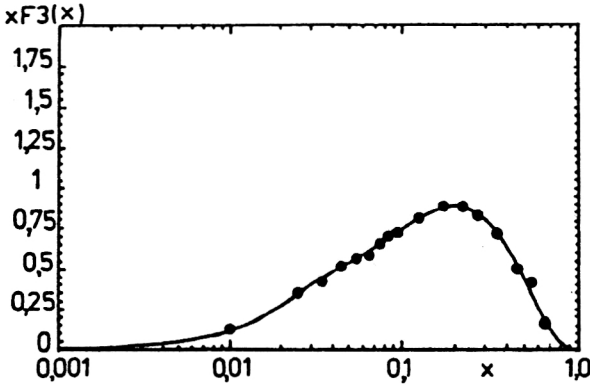


FIG. 9. Description of CCFR data on the structure function $xF_3^{\nu N}(x)$.

However, in the model of the QCD vacuum as an instanton liquid³⁷ we have for $Q_0 > Q > 1/\rho_c$ an instanton contribution to the quark distribution functions corresponding to the substitution $\alpha_s(Q^2) \rightarrow \alpha_s(\rho_c^{-2})$ in (57) and the leading twist in the structure functions.⁵⁹ Unfortunately, the exact dependence of the instanton-induced cross section on the energy is not known. This is due to the fact that at high energies the instantons begin to overlap, and therefore it is necessary to take into account accurately their interaction.

The simplest parametrization is^{51,59}

$$\sigma_{q\bar{q}} \sim s^{\alpha_A - 1} \text{ with } \alpha_A \approx 1, \quad (58)$$

which corresponds to a rapid approach of the instanton cross section to the geometric limit:

$$\sigma_{q\bar{q}}^{\text{inst}} \approx \pi \rho_c^2. \quad (59)$$

At ultrahigh energies, we expect an exponential suppression of the instanton-induced interaction.⁵⁷

Using the relation (56) at small x_0 , we obtain the following form for the function $f(x)$:

$$f(x) \sim \begin{cases} \frac{1}{x} & \text{for } x \geq x_0, \\ \exp(-x_0/x) & \text{for } x < x_0, \end{cases} \quad (60)$$

where x_0 is the value of the Bjorken variable at which the instanton contribution begins to decay rapidly. In accordance with its physical meaning, it must be related to the height of the energy barrier that separates the two topologically non-trivial QCD vacua with $\Delta Q = \pm 1$, i.e., to the so-called sphaleron energy $E_{\text{Sph}}^{\text{QCD}}$ (Ref. 59):

$$x_0 \approx \frac{Q^2}{Q^2 + (E_{\text{Sph}}^{\text{QCD}})^2}. \quad (61)$$

Thus, the final form for $f(x)$ is

$$f(x) = \begin{cases} \frac{N_1}{x} (1-x)^5 & \text{for } x \geq x_0, \\ N_2 \exp(-x_0/x) & \text{for } x < x_0. \end{cases} \quad (62)$$

To calculate the structure functions, we must also specify the valence quark distribution functions and the perturbative quark sea. They were chosen in the standard form:

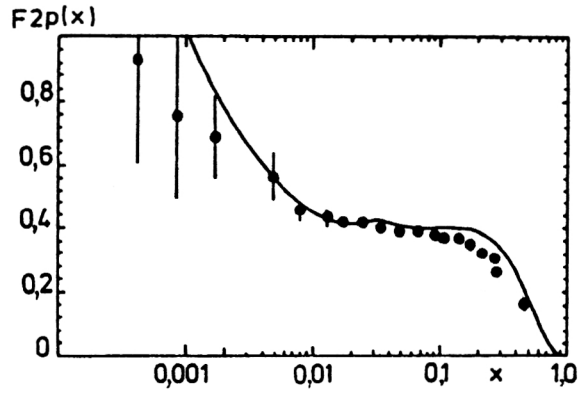


FIG. 10. Description of NMC and H1 data on the structure function $F_2^p(x)$ for $Q^2 = 5 \text{ GeV}^2$.

$$u_v(x) = N_u x^{-\alpha_v} (1-x)^3, \quad d_v(x) = N_d x^{-\alpha_v} (1-x)^4, \\ \bar{q}(x) = N_s (1-x)^7 / x^{\alpha_P(0)}, \quad (63)$$

where $\alpha_P(0)$ is the Pomeron intercept.

The polarization of the valence quarks was chosen to be the same as in the Carlitz-Kaur model.⁶⁰

$$\Delta u_v(x) = u_v(x) - \frac{2}{3} d_v(x), \quad \Delta d_v(x) = -\frac{1}{3} d_v(x). \quad (64)$$

The results of a calculation of the unpolarized and polarized structure functions are presented in Figs. 9–14. The five free parameters were determined by a fit to the unpolarized data, and therefore the calculations of the polarized structure functions were effectively parameter-free. As we see, the model gives an excellent description of all the experimental data on the structure functions. The instantons make a large negative contribution to the spin-dependent structure function $g_1^p(x, Q^2)$, and this makes it possible to explain the anomalous deviation of the experimental points from the prediction of the valence quark model. The amount of helicity carried by the quarks in the nucleon depends strongly on the value of the parameter x_0 , which is determined by the height of the

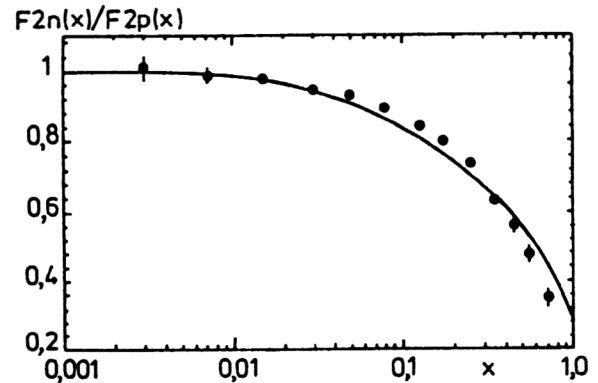


FIG. 11. Description of NMC data on the structure-function ratio $F_2^n(x)/F_2^p(x)$ for $Q^2 = 5 \text{ GeV}^2$.

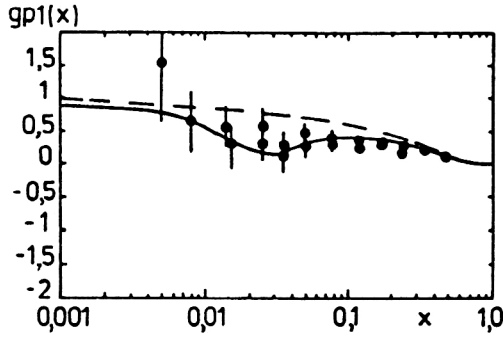


FIG. 12. Description of the EMC and SMC data on the spin-dependent structure function $g_1^p(x)$. The solid curve is the result of a calculation in accordance with the instanton model, and the dashed curve is the prediction of the three-quark valence model.

potential barrier. For the value $x_0=0.032$ obtained from the fit to the unpolarized structure functions the value of the helicity is

$$\Delta\Sigma=0.4. \quad (65)$$

The reduction in (65) relative to its OZI value $\Delta\Sigma^{\text{OZI}}=0.58$ is determined by the instanton-induced anomalous polarization of the quarks: $\Delta\Sigma^{\text{inst}}=-0.18$.

Thus, in the framework of the model of the QCD vacuum as an instanton liquid we have obtained a parametrization of the distribution functions of the quarks in the nucleon that can be used not only to calculate the structure functions of deep inelastic scattering but also to calculate polarized and unpolarized hadronic processes.

CONCLUSIONS

The experimental data on the spin-dependent structure functions obtained by the EMC, SMC, E-142, and E-143 collaborations have led to a crisis of the naive parton model for deep inelastic scattering. We have shown that in QCD this crisis can be resolved by taking into account the compli-

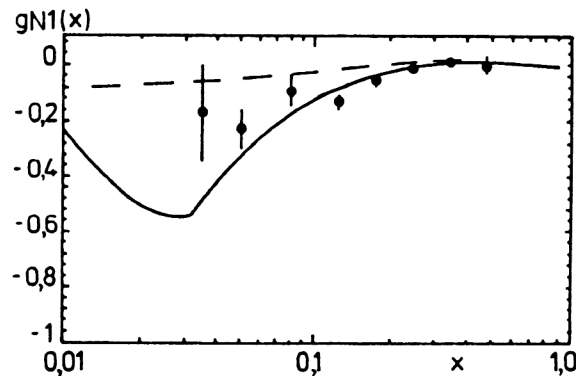


FIG. 13. Description of E-142 data on the spin-dependent structure function $g_1^p(x)$. The solid curve is the result of a calculation in accordance with the instanton model, and the broken curve is the prediction of the three-quark valence model.

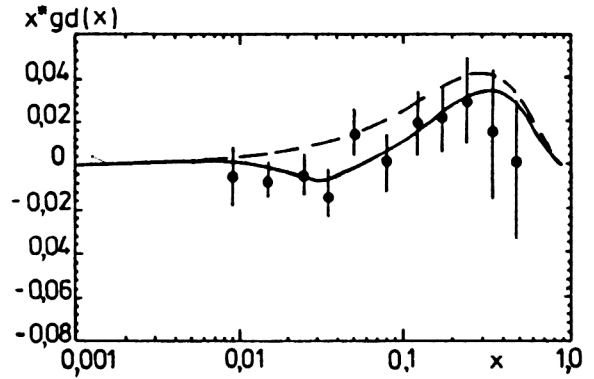


FIG. 14. Description of SMC data on the spin-dependent structure function $g_1^D(x)$. The solid curve is the result of a calculation in accordance with the instanton model, and the dashed curve is the prediction of the three-quark valence model.

cated structure of the QCD vacuum. Thus, the model of the QCD vacuum as an instanton liquid makes it possible, at least qualitatively, to explain the anomalous polarization of the quark sea and its strong flavor asymmetry.

At the same time, the specific flavor and chiral properties of the instanton-induced interaction, and also its anomalous dependence on the energy and momentum transfer, make it the most probable candidate for the fundamental QCD mechanism of spin and flavor effects in deep inelastic scattering and in high-energy hadronic processes.

We are grateful to and thank A. M. Baldin, G. Bunce, P. N. Bogolyubov, G. Brown, S. Brodsky, S. B. Gerasimov, B. Jaffe, A. V. Efremov, L. Kaptar', A. Kotikov, É. A. Kuraev, O. V. Teryaev, T. Thomas, A. Umnikov, and É. Shuryak for valuable discussions.

- ¹ R. L. Jaffe and A. Manohar, Nucl. Phys. **B337**, 509 (1990) and references therein.
- ² S. D. Bass and A. W. Thomas, Adelaide University Preprint ADP-93-218/T136 (1993).
- ³ E. Reya, Dortmund University Preprint DO-TH 93/09 (1993).
- ⁴ B. L. Ioffe, ITEP Preprint 61-94 (1994).
- ⁵ A. E. Dorokhov, N. I. Kochelev, and Yu. A. Zubov, Int. J. Mod. Phys. **A8**, 603 (1993).
- ⁶ A. D. Krish, in *Proc. of the Ninth Intern. Symposium on High Energy Spin Physics* (Bonn, 1990), p. 20.
- ⁷ A. Yokosawa, in *Proc. of the Polarized Collider Workshop* (University Park, 1990), p. 129.
- ⁸ G. G. Bunce *et al.*, Part. World **3**, 1 (1992).
- ⁹ EMC Collaboration (J. Ashman *et al.*), Phys. Lett. **206B**, 364 (1988); Nucl. Phys. **B328**, 1 (1990).
- ¹⁰ B. L. Ioffe, V. A. Khose, and L. N. Lipatov, *Hard Processes*, Vol. 1 (North-Holland, Amsterdam, 1984), p. 61.
- ¹¹ SMC Collaboration (R. Windmalders), in *Report on the SPIN 94 Conference* (Bloomington, 1994).
- ¹² E-143 Collaboration (D. Day), in *Report on the SPIN 94 Conference* (Bloomington, 1994).
- ¹³ G. Altarelli, P. Nason, and G. Ridolfi, Phys. Lett. **320B**, 152 (1994).
- ¹⁴ F. E. Close and R. G. Roberts, Phys. Lett. **316B**, 165 (1993).
- ¹⁵ F. E. Close and R. G. Roberts, RAL Report RAL-94-071 (1994); A. E. Dorokhov and N. I. Kochelev, Phys. Lett. **259B**, 335 (1991).
- ¹⁶ L. P. Kaptari, K. Yu. Kazakov, and A. Yu. Umnikov, Phys. Lett. **293B**, 219 (1992); F. C. Khanna and A. Yu. Umnikov, Phys. Rev. C **49**, 2311 (1994).
- ¹⁷ A. W. Thomas, in *Report on the SPIN 94 Conference* (Bloomington, 1994).

- ¹⁸S. A. Larin and J. A. M. Vermaseren, Phys. Lett. **259B**, 345 (1991); S. A. Larin, Preprint CERN-TH 7208/94 (1994).
- ¹⁹J. Ellis and M. Karliner, Phys. Lett. **313B**, 131 (1993).
- ²⁰J. D. Bjorken, Phys. Rev. **148**, 1467 (1966); Phys. Rev. D **1**, 1376 (1971).
- ²¹J. Ellis and M. Karliner, Preprint CERN-TH 7324/94 (1994).
- ²²V. D. Burkert and B. L. Ioffe, Phys. Lett. **296B**, 223 (1992); Zh. Eksp. Teor. Fiz. **105**, 1153 (1994) [JETP **78**, 619 (1994)].
- ²³S. B. Gerasimov, Yad. Fiz. **2**, 598 (1965) [Sov. J. Nucl. Phys. **2**, 430 (1966)]; S. D. Hearn and A. C. Hearn, Phys. Rev. Lett. **16**, 908 (1966).
- ²⁴I. I. Balitsky, V. M. Braun, and A. V. Kolisnechenko, Phys. Lett. **242B**, 245 (1990); **318B**, 648(E) (1993).
- ²⁵S. B. Gerasimov, in *Report on the Relativistic Nuclear Physics and QCD Conference* (Dubna, 1994).
- ²⁶P. N. Bogoliubov, Ann. Inst. Henri Poincaré **8**, 163 (1967).
- ²⁷A. Chodos, R. L. Jaffe, C. B. Thorn, and V. F. Weisskopf, Phys. Rev. D **9**, 3471 (1974).
- ²⁸E. Leader and M. Anselmino, Z. Phys. C **15**, 19 (1982).
- ²⁹C. S. Lam and Bing-An Li, Phys. Rev. D **25**, 683 (1982); A. V. Efremov and O. A. Teryaev, Preprint E2-88-287, JINR, Dubna (1988); G. Altarelli and G. G. Ross, Phys. Lett. **212B**, 391 (1988); R. D. Carlitz, J. C. Collins, and A. H. Mueller, Phys. Lett. **214B**, 229 (1988).
- ³⁰S. L. Adler, Phys. Rev. **177**, 2426 (1969); J. S. Bell and R. Jackiw, Nuovo Cimento **A60**, 47 (1969).
- ³¹A. V. Efremov and A. V. Radyushkin, Phys. Lett. **63B**, 449 (1976).
- ³²S. B. Libby and G. D. Sterman, Phys. Rev. D **18**, 3252 (1978); A. H. Mueller, Phys. Rev. D **18**, 3705 (1978); J. Ellis, M. Karliner, and C. T. Sachrajda, Phys. Lett. **231B**, 497 (1989); E. L. Berger and J. Qiu, Phys. Rev. D **40**, 778, 3128 (1989); G. Altarelli and B. Lampe, Z. Phys. C **47**, 315 (1990); G. T. Bodwin and J. Qiu, Phys. Rev. D **41**, 2755 (1990).
- ³³A. A. Belavin, A. M. Polyakov, A. S. Schwartz, and Yu. S. Tyupkin, Phys. Lett. **59B**, 85 (1975).
- ³⁴S. Forte, Phys. Lett. **224B**, 189 (1989); Nucl. Phys. **B331**, 1 (1990).
- ³⁵A. E. Dorokhov and N. I. Kochelev, Mod. Phys. Lett. **A5**, 55 (1990); Phys. Lett. **245B**, 609 (1990); B. L. Ioffe and M. Karliner, Phys. Lett. **247B**, 387 (1990).
- ³⁶G. 't Hooft, Phys. Rev. D **14**, 3432 (1976); Phys. Rep. **142**, 357 (1986).
- ³⁷E. V. Shuryak, Phys. Rep. **115**, 151 (1984); D. I. Dyakonov and V. Yu. Petrov, Nucl. Phys. **B272**, 457 (1986).
- ³⁸S. Forte and E. V. Shuryak, Nucl. Phys. **B357**, 153 (1991).
- ³⁹E. V. Shuryak, private communication.
- ⁴⁰S. J. Brodsky, J. Ellis, and M. Karliner, Phys. Lett. **206B**, 309 (1988); J. Ellis and M. Karliner, Phys. Lett. **213B**, 73 (1988); T. Cohen and M. K. Banerjee, Phys. Lett. **230B**, 129 (1989); B. A. Li, in *Report on the SPIN 94 Conference* (Bloomington, 1994).
- ⁴¹S. Narison, G. M. Shore, and G. Veneziano, Preprint CERN-TH 7223/94 (1994).
- ⁴²G. Veneziano, Mod. Phys. Lett. **A4**, 1605 (1989); G. M. Shore and G. Veneziano, Phys. Lett. **224B**, 75 (1990).
- ⁴³A. E. Dorokhov and N. I. Kochelev, in *Proc. of the SPIN 90 Conference* (Bonn, 1990).
- ⁴⁴N. I. Kochelev, Sov. J. Nucl. Phys. **41**, 291 (1985); A. E. Dorokhov and N. I. Kochelev, Sov. J. Nucl. Phys. **52**, 135 (1990); A. E. Dorokhov, Yu. A. Zubov, and N. I. Kochelev, Sov. J. Part. Nucl. **23**, 522 (1992).
- ⁴⁵S. J. Brodsky, M. Burkardt, and I. Schmidt, Preprint SLAC-PUB-6087 (1994).
- ⁴⁶C. Bourrely and J. Soffer, Mod. Phys. Lett. **A8**, 3 (1993).
- ⁴⁷J. Ellis and R. L. Jaffe, Phys. Rev. D **9**, 1444 (1974).
- ⁴⁸K. Gottfried, Phys. Rev. Lett. **18**, 1154 (1967).
- ⁴⁹NMC Collaboration (D. Allasia *et al.*), Phys. Lett. **249B**, 366 (1990); D. Allasia *et al.*, CERN Report CERN-EP/91-105 (1991).
- ⁵⁰A. Ringwald, Nucl. Phys. **B330**, 1 (1990); O. Espinosa, Nucl. Phys. **B343** (1990).
- ⁵¹N. I. Kochelev, Free University of Berlin Preprint FUB-PH 93-13 (1993).
- ⁵²A. E. Dorokhov and N. I. Kochelev, Phys. Lett. **304B**, 167 (1993).
- ⁵³NA51 Collaboration, in *Report of the Rochester Conference* (Glasgow, 1994).
- ⁵⁴S. J. Brodsky, C. Peterson, and N. Sakai, Phys. Rev. D **23**, 2745 (1981).
- ⁵⁵N. I. Kochelev and M. V. Tokarev, Phys. Lett. **309B**, 416 (1993).
- ⁵⁶I. I. Balitsky and M. G. Ryskin, Phys. Lett. **296B**, 185 (1992).
- ⁵⁷I. I. Balitsky and V. M. Braun, Phys. Rev. D **47**, 1879 (1993); Phys. Lett. **314B**, 237 (1993).
- ⁵⁸S. J. Brodsky, Preprint SLAC-PUB-6068 (1994).
- ⁵⁹N. I. Kochelev, in *Report on the SPIN 94 Conference* (Bloomington, 1994).
- ⁶⁰R. Carlitz and J. Kaur, Phys. Rev. Lett. **38**, 673 (1977).

Translated by J. B. Barbour